High-contrast imaging for weakly diffracting specimens in coherent diffraction imaging

Xingchen Pan (潘兴臣)[1], Suhas P. Veetil[2], Cheng Liu (刘 诚)[1*], Qiang Lin (林 强)[1], and Jianqiang Zhu (朱健强)[1]

[1]*Shanghai Institute of Optics and Fine Mechanics, Chinese Academy of Sciences, Shanghai 201800, China*

[2]*Department of Physics, Amity University Dubai, Dubai 345019, United Arab Emirates*

[*]*Corresponding author: chengliu@siom.ac.cn*

Received June 8, 2012; accepted August 7, 2012; posted online January 21, 2013

Coherent diffraction imaging (CDI) and ptychography techniques bypass the difficulty of having high-quality optics in X-ray microscopy by using a numerical reconstruction of the image that is obtained by inverting the diffracted intensity recorded by a charge-coupled device array. However, the reconstruction of the image from the intensity data obtained from a weakly diffracting specimen is known to be difficult because of the obvious reduction in signal-to-noise ratio (SNR). In this case, the specimen only slightly modifies the probe diffraction pattern, resulting in difficulty in the identification of the detailed structure of the specimen from the reconstructed image because of the poor contrast and sharpness of the image. To address this situation, a modification in the image retrieval algorithms used in the iterative reconstruction of the image is suggested. This modification should double the presence of high spatial frequencies in the diffraction pattern to enhance the contrast and edge detection in existing imaging techniques.

OCIS codes: 110.3010, 050.1970, 070.0070.

doi: 10.3788/COL201311.021103.

Recent advances in transmission microscopy have facilitated the evolution of the "lens less" technique for the two-dimensional (2D) or the three-dimensional (3D) reconstruction of the image of nanoscale structures such as proteins, nanotubes, nanocrystals, defects, and so on. The technique is widely known as coherent diffractive imaging (CDI)[1−5]. In this method, the objective lens is removed and a detector is placed in the far-field. Calculating the object structure remains possible through certain iterative phase retrieval algorithms[2−6] despite the loss of all phase information. The object must have finite size, and the sampling condition in the diffraction plane must be satisfied. In the actual optical setup, the object is illuminated by a spatially narrow and well-defined parallel beam of light. Under parallel beam illumination, the intensity of the far-field diffraction patterns is mathematically proportional to the square of the Fourier transform of the transmission function of the object, and the digitized diffraction patterns of the transmission function of the object can be numerically reconstructed iteratively. This theory is the basic principle of the CDI algorithm. Theoretically, CDI allows one to achieve a resolution ultimately limited only by the wavelength of the radiation used, and not by the quality of the optics. Owing to this great advantage, CDI became favoured by researchers in the field of imaging with X-ray and electrons[6−8].

One important advantage of the CDI algorithm is its ability to measure the phase distribution directly from the intensity of the far-field diffraction patterns. For weakly diffracting samples, however, the contrast of the reconstructed phase image is very low, and the fine details in the specimen structure are difficult to see because of the presence of noise. Thus, exploring new methods to enhance the image contrast becomes very meaningful. In this letter, by using diverging illumination for data recording, we proposed a modified ptychographical iterative engine (PIE) algorithm[9−11] for remarkable contrast enhancement. The results obtained can extended to other CDI techniques in practical experiments.

The proposed algorithm for improved contrast of images is a modification of the PIE algorithm[9−11] that can be classified as a reconstruction algorithm that can recover complex value transmission functions of the specimen from a set of ptychographic data. The optical setup used is schematically shown in Fig. 1, where the specimen with a transmission function $q(r)$ is fixed on a translation stage and is illuminated by a complex value illuminating probe wave front $P(r)$. We can also define an exit wave—the wave exiting the specimen—as: $\psi_{\rm e}(r,R) = q(r)P(r-R)$, which is the overlap of the specimen transmission function and the probe function. A charge-coupled device (CCD) array detector was used to receive the far-field intensity of the scatted beam $I(k)$. At the detector, we can measure the intensity of the diffraction pattern by $I(k) = |{\rm FFT}[\psi_{\rm e}(r)]|^2$, where k is the reciprocal space coordinates of the direct space coordinate r.

The far-field intensities were recorded for different sample-to-probe positions, shifted by a vector R. Phase retrieval is started with a random guess of the transmission function $q(r)$. The detailed iteration reconstruction procedure can be found in Ref. [9]. Given that the diffraction pattern is obtained by the interference between the zero-order beam $\mathbf{A}_0(k)$ and the diffracted beam $\mathbf{A}_{\rm d}(k)$, the intensity of the diffraction pattern can be written as

$$I(k) = |\mathbf{A}_0(k) + \mathbf{A}_{\rm d}(k)|^2 = |\mathbf{A}_0(k)|^2 + 2\,|A_0(k)|\,|A_{\rm d}(k)|\cos[\varphi(k)] + |A_{\rm d}(k)|^2 . \quad (1)$$

The phase difference between the zero-order beam and the diffraction beam is $\varphi(k)$. If we assume the phase of

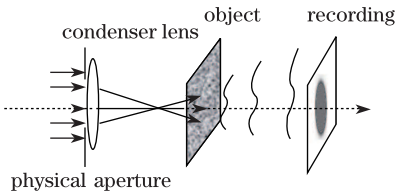

Fig. 1. Optical setup used for the recording of the diffraction pattern by using a diverging beam.

the zero-order beam to be zero, then $\varphi(k)$ is the phase of the diffraction beam.

In the reconstruction process of CDI, the object wave is firstly propagated from the object plane to the recording plane by using the Fresnel formula. On the recording plane, the modulus of the wave is replaced by the square root of the recorded intensity $I^{1/2}(k)$. Then, the wave is inversely propagated back to the object plane and is updated there. These forward and backward propagations are repeated until the accurate image is reconstructed. Mathematically, the diffraction patterns in the far-field plane can be decomposed into different spatial frequency components, and the reconstruction process involves the recombination of different spatial components in real space. By using the intensity $I(k)$, instead of $I^{1/2}(k)$, to update the wave function on the recording plane in each step of computation, a reconstruction, proportional to $\mathbf{A}_0(k)+2\mathbf{A}_\mathrm{d}(k)$, is obtained as

$$\begin{aligned} I^2(k) &= |A_0(k)|^4 + |A_\mathrm{d}(k)|^4 \\ &+ 4\,|A_0(k)|^2\,|A_\mathrm{d}(k)|^2\cos^2[\varphi(k)] + 4(|A_0(k)|^2 \\ &+|A_\mathrm{d}(k)|^2)A_\mathrm{d}(k)A_0(k)\cos[\varphi(k)]+2\,|A_0(k)|^2\,|A_\mathrm{d}(k)|^2 \\ &= |A_0(k)|^4\left(1+\frac{|A_\mathrm{d}(k)|^4}{|A_0(k)|^4}\right)+4\,|A_0(k)|^2\,|A_\mathrm{d}(k)|^2 \\ &+ 4\,|A_0(k)|^3\,|A_\mathrm{d}(k)| \\ &\cdot\left\{\left(1+\frac{|A_\mathrm{d}(k)|^2}{|A_0(k)|^2}\right)\cos[\phi(k)]+\frac{1}{2}\frac{|A_\mathrm{d}(k)|}{|A_0(k)|}\cos[2\varphi(k)]\right\}. \end{aligned} \tag{2}$$

For a weakly diffracting specimen, the zero-order beam is much stronger than the diffracted beam (i.e., $|A_\mathrm{d}(k)| << |A_0(k)|$ and $|A_\mathrm{d}(k)/|A_0(k)| \approx 0$, and Eq. (2) can be simplified as

$$\begin{aligned} I^2(k) &= |A_0(k)|^4 + 4\,|A_0(k)|^2\,|A_\mathrm{d}(k)|^2 \\ &+ 4\,|A_0(k)|^3\,|A_\mathrm{d}(k)|\cos[\varphi(k)] = |A_0(k)|^2\,(|A_0(k)|^2 \\ &+ 4\,|A_\mathrm{d}(k)|^2 + 4\,|A_0(k)|\,|A_\mathrm{d}(k)|\cos[\varphi(k)]) \\ &= |A_0(k)|^2\,|\mathbf{A}_0(k)+2\mathbf{A}_\mathrm{d}(k)|^2, \end{aligned} \tag{3}$$

where the strength of the diffracted beam $\mathbf{A}_\mathrm{d}(k)$, which indicates the high spatial frequency components of the object wave, is doubled, relative to the zero-order beam, while considering $I(k)$ instead of $I(k)^{1/2}$. According to the principles of Fourier optics, the contrast of this reconstruction will be remarkably enhanced for both the phase and intensity images.

To show this condition clearly, we draw the vectors of $\mathbf{A}_0(k)+\mathbf{A}_\mathrm{d}(k)$ and $\mathbf{A}_0(k)+2\mathbf{A}_\mathrm{d}(k)$ in the complex plane in Fig. 2, where we assume the polar angle of the zero-order component $\mathbf{A}_0(k)$ to be zero and the polar angle $\mathbf{A}_\mathrm{d}(k)$ to be $\varphi(k)$. Evidently, $\mathbf{A}_0(k)+2\mathbf{A}_\mathrm{d}(k)$ has longer vector length and larger polar angle than $\mathbf{A}_0(k)+\mathbf{A}_\mathrm{d}(k)$, resulting in $\beta > \alpha$, which indicates that the reconstruction using the proposed method will result in a wide phase range. Such a wide phase range is desirable because the probe diffraction pattern is only slightly modified by the weakly diffracting specimen. This method causes the phase change to be very conspicuous, resulting in better contrast and visual information of the specimen.

The validity of the foregoing analysis is verified in a numerical simulation. Figure 3(a) is the phase transmit function of a pure phase object chosen for simulation. Figure 3(b) is the intensity of the far-field diffraction patterns calculated. As diverging illumination was used and the object was quite weakly diffracting, the zero-order beam occupied a large portion of the area in Fig. 3(b), which is required for the assumption that $|A_\mathrm{d}(k)| << |A_0(k)|$. To simulate a practical experimental situation, some random noise (e.g., dark current CCD noise) was added to the diffraction pattern. Figure 3(c) is the reconstruction with the common PIE method, using the square root of intensity obtained in Figure 3(b). The structural information of the object was lost in the dominant noise. Figure 3(d) is the image reconstructed by using our modified algorithm. It shows the phase structure of Fig. 3(a). For comparison, the phase profiles along the dashed lines in Figs. 3(a) and (d) are shown in Fig. 4, with a red dotted line and a blue solid line, respectively. The phase distributions in Figs. 3 and 4 are the phase changes in the light transmitting the sample, which is

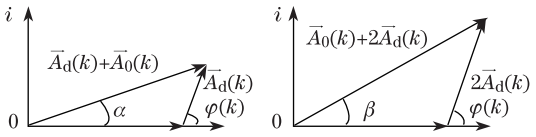

Fig. 2. $\overrightarrow{A_0}(k)+\overrightarrow{A_\mathrm{d}}(k)$ and $\overrightarrow{A_0}(k)+2\overrightarrow{A_\mathrm{d}}(k)$ in complex plane.

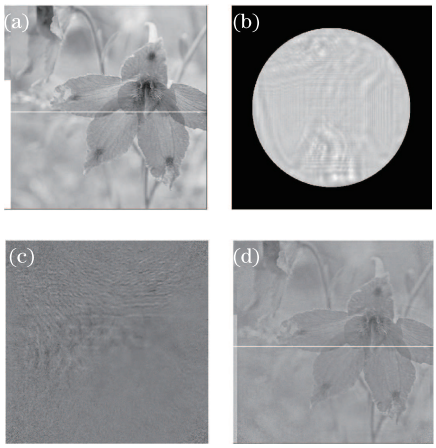

Fig. 3. Numerical simulation results of (a) phase transmission of the object, (b) diffraction pattern, (c) reconstructed image with common PIE method, and (d) reconstructed image by using our method.

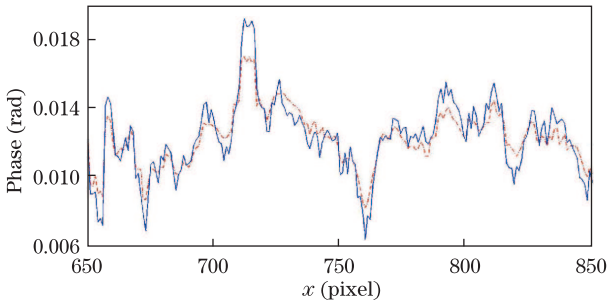

Fig. 4. (Color online) Original phase (dotted line) and reconstructed phase (solid line) with modified algorithm. The phase profiles are taken along the dash lines in Figs. 3(a) and (d).

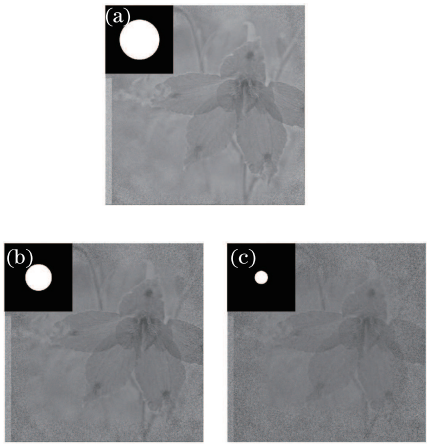

Fig. 5. Reconstructed images of phase object with smaller numerical apertures while the numerical apertures are (a) three-fourth, (b) one-half, and (c) one-fourth of those shown in Fig. 3(b).

slightly different from the common spatial phase distribution of a light field. The reconstruction of the weak phase object using the square root of the intensity patterns was difficult because of the noise added to the patterns. The modified algorithm that we propose can faithfully reproduce the structures of objects, demonstrating high degree of noise tolerance and improved contrast. The simulation results very well matched the reconstruction method outlined in this letter.

For illumination with small numerical apertures, the zero-order disk covers only a small portion of the CCD target. For the most part of the recorded data, Eq. (3) does not apply. Thus, the proposed method is invalid. To show this clearly, we also performed some simulations with small numerical apertures. The reconstructed results, along with the apertures, are shown in Figs. 5(a), (b), and (c). The numerical apertures were only three-fourth, one-half, and one-fourth of that shown in Fig. 3(b), respectively. As the numerical aperture decreased, the details of the object were lost, and obvious distortion was observed. Reconstruction can also be done using the cubic of the modulus of the recorded data $I^{3/2}(k)$, to further enhance the image contrast. However, the contrast cannot be sharpened infinitely, because as the strength of the diffraction beam changes from $\mathbf{A}_{\rm d}(k)$ to $2\mathbf{A}_{\rm d}(k)$, $3\mathbf{A}_{\rm d}(k)\cdots$, and so on, it becomes closer in intensity to $\mathbf{A}_0(k)$ and the condition $|\mathbf{A}_{\rm d}(k)| << |\mathbf{A}_0(k)|$ in Eq. (3) will not be satisfied.

In the foregoing analysis, only the random noise, which corresponds to the readout noise of CCD array, was used for the simulations discussed. However, simulations with other types of noise, including Poisson's noise, showed same results. Conversely, although standard PIE algorithm was used to demonstrate the feasibility of our proposed method, extended PIE[12] also works well with our proposed method. For clarity, however, these hypotheses were not analyzed here.

Several samples used in electron or X-ray microscopy have weak scattering, and the reconstruction of such samples always suffer from low image quality. In search of better image contrast for PIE and other CDI techniques for the imaging of weakly scattering objects, an optical setup for data recording and a corresponding algorithm for image reconstruction are proposed in this letter. The strength of the diffraction beam was doubled, compared with the common algorithms used in CDI techniques, and the image contrast was obviously enhanced. The results of this letter also explained a phenomenon that has confused researchers for a long time. Although the CDI imaging theory requires using the square root of the recorded data $I^{1/2}(k)$, in practical experiments involving X-ray imaging, a reconstruction with $I^{n/2}(k)$ can produce better contrast in some cases. Here, n can be 1.2, 1.3, or other values slightly greater than 1.0. This letter explains the underlying physics of such a reconstruction, which enhances the visual information of a specimen to a great extent.

This work was supported by the One Hundred Person Project of Chinese Academy of Sciences under Grant No. 1104331-JR0.

References

1. J. Miao, C. Charalambous, J. Kirz, and D. Sayre, Nature **400,** 342 (1999).
2. U. Weierstall, Q. Chen, J. Spence, M. Howells, M. Isaacson, and R. Panepucci, Ultramicroscopy **90,** 171 (2001).
3. J. R. Fienup, Appl. Opt. **21,** 2758 (1982).
4. J. Spence, U. Weierstall, and M. Howells, Philos. Trans. **360,** 875 (2002).
5. H. He, S. Marchesini, M. Howells, U. Weierstall, G. Hembree, and J. C. H. Spence, Acta. Cryst. A **59,** 143 (2003).
6. D. Shapiro, P. Thibault, T. Beetz, V. Elser, M. Howells, C. Jacobsen, J.Kirz, E. Lima, H. Miao, A. M. Neiman, and D. Sayre, Proc. Natl. Acad. Sci. USA **102,** 15343 (2005).
7. M. A. Pfeifer, G. J. Williams, I. A. Vartanyants, R. Harder, and I. K. Robinson, Nature **442,** 63 (2006).
8. H. N. Chapman, A. Barty, S. Marchesini, A. Noy, S. P. Hau-Riege, C. Cui, M. R. Howells, R. Rosen, H. He, J. C. H. Spence, U. Weierstall, T. Beetz, C. Jacobsen, and D. Shapiro, J. Opt. Soc. Am. A **23,** 1179 (2006).
9. J. M. Rodenburg, Adv. Imag. Electron. Phys. **150,** 87 (2008).
10. J. M. Rodenburg, A. Hurst, and A. Cullis, Ultramicroscopy **107,** 227 (2007).
11. J. M. Rodenburg, A. C. Hurst, A. G. Cullis, B. R. Dobson, F. Pfeiffer, O. Bunk, C. David, K. Jefimovs, and I. Johnson, Phys. Rev. Lett. **98,** 034801 (2007).
12. A. M. Maiden and J. M. Rodenburg, Ultramicroscopy **109,** 1256 (2009).